Another method to compute the thermodynamic Casimir force in lattice models

Martin Hasenbusch*
Institut für Physik, Humboldt-Universität zu Berlin, Newtonstr. 15, 12489 Berlin, Germany
(Received 3 September 2009; published 16 December 2009)

We discuss a method that allows us to compute the thermodynamic Casimir force at a given temperature in lattice models by performing a single Monte Carlo simulation. It is analogous to the one used by de Forcrand and co-workers in the study of 't Hooft loops and the interface tension in SU(N) lattice gauge models in four dimensions. We test the method at the example of thin films in the XY universality class. In particular we simulate the improved two-component ϕ^4 model on the simple cubic lattice. This allows us to compare with our previous study, where we have computed the Casimir force by numerically integrating energy densities over the inverse temperature.

DOI: 10.1103/PhysRevE.80.061120 PACS number(s): 05.50.+q, 05.70.Jk, 05.10.Ln

I. INTRODUCTION

In 1978 Fisher and de Gennes [1] realized that when thermal fluctuations are restricted by a container a force acts on the walls of the container. Since this effect is similar to the Casimir effect, where the restriction of quantum fluctuations induces a force, it is called "thermodynamic" Casimir effect. Since thermal fluctuations only extend to large scales in the neighborhood of a continuous phase transition it is also called "critical" Casimir effect. For reviews on critical phenomena and the renormalization group, see, e.g., [2–5]. Recently the thermodynamic Casimir effect has attracted much attention since it could be verified for various experimental systems and quantitative predictions could be obtained from Monte Carlo simulations of spin models [6]. The neighborhood of the critical point implies that the Casimir force is described by a universal finite size scaling (FSS) [7,8] function. For the film geometry, finite size scaling predicts

$$F_{Casimir}(L_0,t) \simeq \frac{k_B T}{L_0^3}\theta(t[L_0/\xi_0]^{1/\nu}), \tag{1}$$

where k_B is the Boltzmann constant, T is the temperature, $t=(T-T_c)/T_c$ is the reduced temperature, and L_0 is the thickness of the film. The amplitude ξ_0 of the correlation length in the high-temperature phase is defined by

$$\xi \simeq \xi_0 t^{-\nu}, \tag{2}$$

where ξ is the correlation length of the bulk system and ν is its critical exponent. The function $\theta(x)$ is the same for all films in a given universality class, where also the boundary universality class [9] has to be taken into account.

As a first application of the numerical method discussed here, we study the improved two-component ϕ^4 model on the simple cubic lattice. The phase transition of this model belongs to the XY universality class in three dimensions. Also the λ transition of ^{4}He shares this universality class. The experimental study of the λ transition provided highly accurate estimates for critical exponents and amplitude ratios of the bulk system. For a review see [10]. Also confined systems have been studied in detail at the λ transition of ^{4}He [11]. In particular, the thermodynamic Casimir force in thin films of ^{4}He has been measured [12,13]. These experiments confirm that the thermodynamic Casimir force for films of different thicknesses L_0 can indeed be described by the same scaling function $\theta(x)$. For all temperatures the force turns out to be attractive. In the high-temperature phase $\theta(x)$ is monotonically decreasing with decreasing x. The Casimir force vanishes for large values of x. At the critical point of the bulk system $\theta(0)=-0.07\pm0.03$ [12]. In the low-temperature phase the finite size scaling function shows a minimum at $x_{min}\approx-5.5$ with $\theta_{min}\approx1.3$ [13]. For $x<x_{min}$ the finite size scaling function increases with decreasing temperature. For small values of x it seems to approach a finite negative value.

It has been a long-standing challenge for theorists to compute the finite size scaling function $\theta(x)$: Krech and Dietrich [14,15] computed it in the high-temperature phase using the ϵ expansion up to $O(\epsilon)$. This result is indeed consistent with the measurements on ^{4}He films. Deep in the low-temperature phase, the spin wave approximation should provide an exact result. It predicts a negative nonvanishing value for $\theta(x)$. However the experiments suggest a much larger absolute value for $\theta(x)$ in this region. Using a renormalized mean-field approach Zandi *et al.* and Maciolek *et al.* [16,17] computed $\theta(x)$ for the whole temperature range. Qualitatively they reproduced the features of the experimental result. However the position of the minimum is almost a factor of 2 different from the experimental one. The value at the minimum is wrongly estimated by a factor of about 5.

Only quite recently Monte Carlo simulations of the XY model on the simple cubic lattice [18–20] provided results for $\theta(x)$ which essentially reproduce the experiments on ^{4}He films [12,13]. In [21] we have applied the method used in [18] to study the improved two-component ϕ^4 model on the simple cubic lattice. The study of this model should provide more accurate results since corrections $\propto L_0^{-\omega}$ with $\omega=0.785(20)$ [22] are eliminated. Essentially our result confirms those in [18–20]. However there is a discrepancy in the position x_{min} of the minimum of $\theta(x)$ that is clearly larger than the errors that are quoted: in [18] $x_{min}=-5.3(1)$ and in [20] $x_{min}=-5.43(2)$ which has to be compared with our result $x_{min}=-4.95(3)$ [21].

In order to complement and, to some extend, verify our result for $\theta(x)$ [21] we compute the thermodynamic Casimir

*martin.hasenbusch@physik.hu-berlin.de

force in the two-component ϕ^4 model using a different method that is analog to that in [23,24] used to compute the string tension and 't Hooft loops in lattice gauge model. The general idea is similar to that in [19,20]. In contrast to [19,20], provided that f_{bulk} is known, a single simulation is sufficient to obtain the Casimir force at a given temperature.

This paper is organized as follows. First we define the ϕ^4 model on the simple cubic lattice. Then in Sec. III we discuss in detail the method used here to compute the thermodynamic Casimir force. In Sec. IV we discuss our numerical simulations. First we performed numerical simulations at the critical point of the three-dimensional system. Next we computed the free energy density for the thermodynamic limit of the three-dimensional system at two values of the inverse temperature β in the high and the low-temperature phase each. Then we have measured the thermodynamic Casimir force for $L_0=8.5$ at various temperatures. Finally we have simulated at x_{min}, which we already had computed in Ref. [21] for the thicknesses $L_0=6.5$, 7.5, 9.5, 12.5, and 24.5 to complement our results for the thermodynamic Casimir force at its minimum. Finally we summarize our results and give our conclusion.

II. MODEL AND OBSERVABLES

We study the two-component ϕ^4 model on the simple cubic lattice. We label the sites of the lattice by $x=(x_0,x_1,x_2)$. The components of x may assume the values $x_i \in \{1,2,\ldots,L_i\}$. Throughout we simulate lattices of the size $L_1=L_2=L$ and mostly $L_0 \ll L$. In one and two directions periodic boundary conditions are used. In order to mimic the vanishing order parameter that is observed at the boundaries of ^{4}He films, free boundary conditions in zero direction are employed. This means that the sites with $x_0=1$ and $x_0=L_0$ have only five nearest neighbors. This type of boundary conditions could be interpreted as Dirichlet boundary conditions with 0 as value of the field at $x_0=0$ and $x_0=L_0+1$. Note that viewed this way, the thickness of the film is L_0+1 rather than L_0. This provides a natural explanation of the result $L_s=1.02(7)$ obtained in [25]. The Hamiltonian of the two-component ϕ^4 model, for a vanishing external field, is given by

$$\mathcal{H}=-\beta\sum_{\langle x,y\rangle}\vec{\phi}_x\cdot\vec{\phi}_y+\sum_x[\vec{\phi}_x^2+\lambda(\vec{\phi}_x^2-1)^2], \tag{3}$$

where the field variable $\vec{\phi}_x$ is a vector with two real components. $\langle x,y\rangle$ denotes a pair of nearest-neighbor sites on the lattice. The partition function is given by

$$Z=\prod_x\left[\int d\phi_x^{(1)}\int d\phi_x^{(2)}\right]\exp(-\mathcal{H}). \tag{4}$$

Note that following the conventions of our previous work, e.g., [26], we have absorbed the inverse temperature β into the Hamiltonian. Therefore, following [4] we actually should call it reduced Hamiltonian. In the limit $\lambda\to\infty$ the field variables are fixed to unit length; hence the XY model is recovered. For $\lambda=0$ we get the exactly solvable Gaussian model. For $0<\lambda\leq\infty$ the model undergoes a second-order phase transition that belongs to the XY universality class. Numerically, using Monte Carlo simulations and high-temperature series expansions, it has been shown that there is a value $\lambda^*>0$, where leading corrections to scaling vanish. We refer to the two-component ϕ^4 model at $\lambda=\lambda^*$ as the improved two-component ϕ^4 model. Numerical estimates of λ^* given in the literature are $\lambda^*=2.10(6)$ [27], $\lambda^*=2.07(5)$ [26], and most recently $\lambda^*=2.15(5)$ [22]. The inverse of the critical temperature β_c has been determined accurately for several values of λ using FSS [22].

We shall perform our simulations at $\lambda=2.1$ since for this value of λ comprehensive Monte Carlo studies of the three-dimensional system in the low- and the high-temperature phases have been performed [22,25,28,29]. At $\lambda=2.1$ one gets $\beta_c=0.509\,150\,3(6)$ [22]. Since $\lambda=2.1$ is not exactly equal to λ^*, there are still corrections $\propto L_0^{-\omega}$, although with a small amplitude. In fact, following [22], it should be by at least a factor 20 smaller than for the standard XY model.

Energy density and reduced free energy

Note that in Eq. (3) β does not multiply the second term. Therefore, strictly speaking, β is not the inverse of k_BT. In order to study universal quantities it is not crucial how the transition line in the β-λ plane is crossed as long as this path is not tangent to the transition line. Therefore, following computational convenience, we vary β at fixed λ. In the following equations it is understood that λ is kept fixed.

The reduced free energy density is defined as

$$f(\beta)\equiv-\frac{1}{L_0L_1L_2}[\ln Z(\beta)-\ln Z(0)]. \tag{5}$$

Note that compared with the free energy density $\tilde{f}$, a factor k_BT is skipped. For convenience we have defined the reduced free energy such that $f(0)=0$. For $\beta=0$ the partition function factorizes and thus $\ln Z(0)/(L_0L_1L_2)$ does not depend on the system size.

We define the (internal) energy density as the derivative of the reduced free energy density with respect to β. Furthermore, to be consistent with our previous work, e.g., [30], we multiply by -1

$$E=\frac{1}{L_0L_1L_2}\frac{\partial\ln Z}{\partial\beta}. \tag{6}$$

It follows

$$E=\frac{1}{L_0L_1L_2}\left\langle\sum_{\langle x,y\rangle}\vec{\phi}_x\cdot\vec{\phi}_y\right\rangle, \tag{7}$$

which can be easily determined in Monte Carlo simulations. From Eqs. (5) and (6) it follows that the free energy density can be computed as

$$f(\beta)=f(\beta_0)-\int_{\beta_0}^{\beta}d\tilde{\beta}E(\tilde{\beta}). \tag{8}$$

III. NUMERICAL METHOD

From a thermodynamic point of view, the Casimir force per unit area is given by

$$F_{Casimir} = -k_B T \frac{\partial f_{ex}}{\partial L_0}, \tag{9}$$

where L_0 is the thickness of the film and $f_{ex}=f_{film}-L_0 f_{bulk}$ is the reduced excess free energy per area of the film. In lattice models the thickness L_0 assumes only integer values. Therefore we have to approximate the derivative by a finite difference $F_{Casimir}(L_0,t) \approx -k_B T \Delta f_{ex}(L_0,t)$, where

$$\Delta f_{ex}(L_0,t) \equiv f(L_0+1/2,t) - f(L_0-1/2,t) - f_{bulk}(t), \tag{10}$$

where $L_0+1/2$ is integer. $f(L_0+1/2,t)$ and $f(L_0-1/2,t)$ are the reduced free energies per area of films of the thicknesses $L_0+1/2$ and $L_0-1/2$, respectively, and $f_{bulk}(t)$ is the reduced free energy density of the three-dimensional bulk system. The main numerical task is to compute the difference of the reduced free energy per area for films of the thicknesses $L_0-1/2$ and $L_0+1/2$.

In order to compute this difference, it is useful to have the same number of field variables for both systems. To this end, we add $L_1 \times L_2$ isolated sites to the film of the thickness $L_0-1/2$. Isolated means that the field $\vec{\phi}$ at such a site is subject to the potential $\vec{\phi}^2+\lambda(\vec{\phi}^2-1)^2$ but the interaction with other sites is missing. Using our definition [Eq. (5)] and adding isolated sites to the film do not change the free energy per area. Let us denote the partition function of this system by $\bar{Z}_{L_0-1/2}$. Now we can express the difference of the reduced free energies as

$$\begin{aligned} &F(L_0+1/2,t) - F(L_0-1/2,t) \\ &= \ln \frac{\bar{Z}_{L_0-1/2}}{Z_{L_0+1/2}} \\ &= \ln \frac{D[\phi] \exp(-H_{L_0+1/2}) \exp\left(-\beta \sum_{\langle x,y\rangle \in [L_0+1/2]} \vec{\phi}_x \vec{\phi}_y\right)}{D[\phi] \exp(-H_{L_0+1/2})} \\ &= \ln \left\langle \exp\left(-\beta \sum_{\langle x,y\rangle \in [L_0+1/2]} \vec{\phi}_x \vec{\phi}_y\right) \right\rangle_{L_0+1/2}, \end{aligned} \tag{11}$$

where $\langle x,y\rangle \in [L_0+1/2]$ denotes the sum over all nearest-neighbor pairs, where at least one of the sites is an element of the layer $x_0=L_0+1/2$. Formally we have rewritten the difference of free energies as an expectation value. The problem is that the observable is strongly fluctuating and therefore it is impossible to obtain an accurate estimate from a Monte Carlo simulation of the film of the thickness $L_0+1/2$. A well known method to overcome this problem is the so called "multistage sampling" strategy; see, e.g., [31]. This means that a sequence of systems is introduced that interpolates between the two we are interested in. These systems are characterized by the Hamiltonians $H_0, H_1, \ldots, H_N$, where we identify $H_0=\bar{H}_{L_0-1/2}$ and $H_N=H_{L_0+1/2}$. Now we can rewrite the ratio of partition functions as

$$\frac{Z_0}{Z_N} = \frac{Z_0}{Z_1}\frac{Z_1}{Z_2} \cdots \frac{Z_{N-1}}{Z_N}, \tag{12}$$

where we can write the factors as

$$z_{i+1} \equiv \frac{Z_i}{Z_{i+1}} = \langle \exp(-H_{i+1}+H_i) \rangle_{i+1} \tag{13}$$

and hence

$$F(L_0+1/2,t) - F(L_0-1/2,t) = \sum_{i=1}^{N} \ln z_i. \tag{14}$$

If the sequence is properly chosen and N is sufficiently large, the fluctuations of $\exp(-H_{i+1}+H_i)$ are small and the expectation value can be accurately determined from the simulation of the system $i+1$. Obviously there is much freedom in the construction of the sequence of systems. A straightforward one is given by

$$H_i = \bar{H}_{L_0-1/2} + \frac{i}{N} \beta \sum_{\langle x,y\rangle \in [L_0+1/2]} \vec{\phi}_x \vec{\phi}_y. \tag{15}$$

This choice is very similar to the one used in [19,20]. The main difference is that these authors did consider as starting system a film of thickness $L_0-1/2$ plus a two-dimensional system of the size $L_1 \times L_2$. This means that in contrast to our choice the intralayer couplings are switched on.

Here we use a different interpolation. It is inspired by a method used to compute the string tension and 't Hooft loops in lattice gauge theories [23,24].

We add the isolated sites one by one to the film. In the step $i=(x_1-1)L_1+x_2$ the site $x=(L_0+1/2,x_1,x_2)$ is added. All sites that are added are coupled with their nearest neighbors that are already in the film. This way we have constructed a sequence of $L_1 \times L_2+1$ systems. Hence, $L_1 \times L_2$ independent Monte Carlo simulations have to be performed to obtain $F(L_0+1/2,t)-F(L_0-1/2,t)$. Following [23,24] this can however be avoided: with increasing L_1, L_2 the sum [Eq. (14)] is dominated by contributions where the newly added site is far from the defect line between $x_1=L_1$ and $x_1=1$ as well as from the point defect between $x_2=L_2$ and $x_2=1$. Hence most of the contributions are essentially equal to that for $x_1=L_1/2$ and $x_2=L_2/2$ as sketched in Fig. 1. In the limit $L_1, L_2 \to \infty$, this should become exact. Hence only a single simulation for $x_1=L_1/2$ and $x_2=L_2/2$ is required.

Usually updates are performed on the whole lattice ("sweep") before a measurement of the observables is performed. However in the present case, the observable is localized at a single site. Therefore the effort for the measurement and the update would be highly unbalanced. To circumvent this problem, one would like to update the fields in the neighborhood of this site more frequently than those far off. In order to achieve this we follow the idea presented in [32]: we consider a sequence of subsets of the sites of the lattice. Here, the smallest set consists of the site $(L_0+1/2, L_1/2, L_2/2)$ only. The next larger one consists of $(L_0+1/2, L_1/2, L_2/2)$ and its three neighbors $(L_0+1/2, L_1/2-1, L_2/2)$, $(L_0+1/2, L_1/2, L_2/2-1)$, and $(L_0-1/2, L_1/2, L_2/2)$. The larger ones are given by blocks of the size $b_l \times (2b_l$

$+1)\times(2b_l+1)$ and $L_0\times(2b_l+1)\times(2b_l+1)$ if $b_l>L_0$. These blocks are centered around the site $(L_0+1/2,L_1/2,L_2/2)$. If $b_l<L_0$, the eight corners of these blocks are $(L_0+1/2,L_1/2-b_l,L_2/2\pm b_l)$, $(L_0-1/2,L_1/2+b_l,L_2/2\pm b_l)$, and $(L_0+1/2\pm b_l,L_1/2-b_l,L_2/2\pm b_l)$. In our simulations we have used $b_l=1,2,3,5,10,20,40,80,\ldots$, where the largest b_l is chosen such that $2b_l+1<L_1,L_2$.

In a certain sequence, Metropolis and over-relaxation sweeps over these subsets are performed. We have implemented these updates as discussed in appendix A in [26]. This sequence, which we shall call one update cycle, is best explained by the following pseudocode

```
cluster_update(); metrosweep(full lattice); oversweep(full lattice);
for(i1=0; i1<m_1; i1++)
  {
  metrosweep (b_1); oversweep (b_1);
  for(i2=0; i2<m_2; i2++)
    {
    metrosweep (b_2); oversweep (b_2);
    .
    .
    .
      for(iM=0; iM<m_M; iM++)
        {
        metrosweep (b_M); oversweep (b_M);
        measure();
    }
    .
    .
    .
    }
    }
```

This means that in one cycle $m_1\times m_2\times\ldots\times m_M$ measurements are performed. We did not accurately tune the parameters $m_1,m_2,m_3,\ldots,m_M$; instead we have chosen them such that the CPU time spent at each block size is roughly the same. This is approximately achieved by choosing $m_l b_l^d=\text{const}$, where d is the dimension of the system.

In the case of the single cluster updates [33] it is easy to focus on the site $(L_0+1/2,L_1/2,L_2/2)$. One simply starts the clusters at the site $(L_0+1/2,L_1/2,L_2/2)$ instead of choosing the starting point at random. In our numerical tests we have not yet implemented this idea.

Measurement

The measurement consists, in its most naive implementation, of the evaluation of

$$A=\exp(-\beta\vec{\phi}_{(L_0+1/2,L_1/2,L_2/2)}\cdot\vec{\Phi}_{(L_0+1/2,L_1/2,L_2/2)}), \quad (16)$$

where

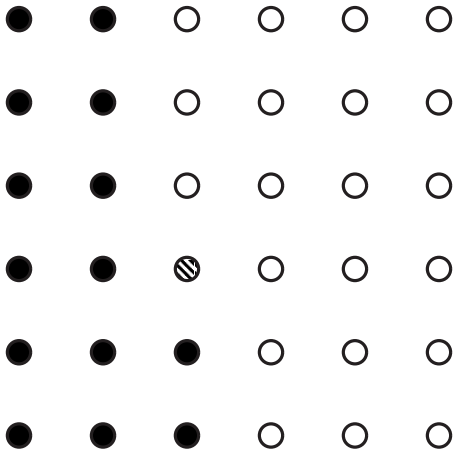

FIG. 1. We sketch the layer $x_0=L_0+1/2$ of our system. In the sketch $L_1=L_2=6$. The sites are given by circles. The filled ones are coupled to the system, while the empty ones are isolated. We compute the free energy difference between the system where the shaded circle is isolated and the system where it is coupled to the film. Note that due to the periodic boundary conditions in one and two directions there is also a defect line between $x_1=1$ and $x_1=L_1$ and a point defect at $L_1/2$ between $x_2=1$ and $x_2=L_2$. For a discussion see the text.

$$\vec{\Phi}_{(L_0+1/2,L_1/2,L_2/2)}=\vec{\phi}_{(L_0+1/2,L_1/2-1,L_2/2)}+\vec{\phi}_{(L_0+1/2,L_1/2,L_2/2-1)}+\vec{\phi}_{(L_0-1/2,L_1/2,L_2/2)}. \quad (17)$$

We have reduced the variance by performing the integral over the angle of the field $\vec{\phi}_{(L_0+1/2,L_1/2,L_2/2)}$ exactly. This results in the improved observable

$$\bar{A}=\frac{1}{\int_0^{2\pi}d\alpha\,\exp(-R\cos\alpha)}=\frac{1}{2\pi I_0(R)}, \quad (18)$$

where

$$R=\beta|\vec{\phi}_{(L_0+1/2,L_1/2,L_2/2)}||\vec{\Phi}_{(L_0+1/2,L_1/2,L_2/2)}| \quad (19)$$

and $I_0(R)$ is a modified Bessel function. For our simulations we have tabulated $1/[2\pi I_0(R)]$ for $0\le R\le 3$ with a step size of 0.0001, i.e., for 30 001 values of R. During the simulation we then evaluated $1/[2\pi I_0(R)]$ for $0\le R\le 3$ by quadratically interpolating the results given in the table. If $R>3$ we have evaluated the integral in Eq. (18) numerically. A sufficient precision can already be achieved with about 30 nodes.

The expectation value

$$z=\langle A\rangle=\langle\bar{A}\rangle \quad (20)$$

is estimated by averaging $\bar{A}$ over all measurements that we performed after thermalization. Here we have dropped the subscript $i=(L_1/2-1)L_2+L_2/2$ of Eq. (13) since only this value of i will be considered in the following. During the simulation we have averaged already all measurements in a given update cycle. These averages were written to a file. The statistical error was then computed taking into account the integrated autocorrelation time of these cycle averages.

TABLE I. Results for z at $\beta_c=0.509\ 150\ 3$ [22] for lattices of the size $L_1=L_2=12.5\times(L_0-1/2)$.

L_0	z
8.5	0.84951552(24)
12.5	0.84947657(16)
16.5	0.84946525(23)
24.5	0.84945897(13)
32.5	0.84945717(16)
64.5	0.84945602(14)

IV. NUMERICAL RESULTS

First we have simulated at the critical temperature of the bulk system. Next we have determined the reduced free energy of the bulk system at $\beta=0.49$ and $\beta=0.5$ in the high-temperature phase and at $\beta=0.533$ and $\beta=0.56$ in the low-temperature phase. For $L_0, L_1, L_2 \gg \xi$ the reduced free energy of the bulk system is given by $f_{bulk}=\ln z$. Our results are consistent with those obtained by integrating the energy densities computed in [30]. Then we have studied films of the thickness $L_0=8.5$ at four temperatures in the low-temperature phase of the bulk system. Also here we find that the results are consistent with those in [30]. Finally we have simulated the thicknesses $L_0=6.5$, 7.5, 9.5, 12.5, and 24.5 at x_{min}. These simulations complement our results in [30] at x_{min}.

As random number generator we have used the SIMD-oriented fast Mersenne twister algorithm [34].

A. Simulations at the critical point

First we performed simulations at the inverse critical temperature $\beta_c=0.509\ 150\ 3(6)$ of the three-dimensional system using lattices of the thicknesses $L_0=8.5$, 12.5, 16.5, 24.5, 32.5, and 64.5. In all cases we have chosen $L_1=L_2=12.5\times(L_0-1/2)$. Since the correlation length of the film is $\xi_{2nd,film}/L_{0,eff}\approx 0.416$ [30] this should be sufficient to keep deviations from the two-dimensional thermodynamic limit smaller than our statistical errors. As a check we have simulated for $L_0=8.5$, in addition $L_1=L_2=20$, 30, and 50. We find $z=0.849\ 505\ 17(36)$, $0.849\ 513\ 62(36)$, and $0.849\ 515\ 72(37)$ for these lattice sizes, respectively. Indeed, starting from $L_1=L_2=50$ our results are consistent within error bars. Our results for $L_1=L_2=12.5\times(L_0-1/2)$ are summarized in Table I. In these simulations we have used block sizes up to $b_1=10$, 20, 20, 40, 40, and 80 for $L_0=8.5$, 12.5, 16.5, 24.5, 32.5, and 64.5, respectively. For all these thicknesses and for all block sizes we have used $m_l=6$. The numbers of update cycles are 2.1×10^7, 7.7×10^6, 7.7×10^6, 2×10^6, 1.3×10^6, and 2.8×10^5 for $L_0=8.5$, 12.5, 16.5, 24.5, 32.5, and 64.5, respectively. In total these simulations took about 16 month of CPU time on a single core of a quad-core Opteron(tm) 2378 CPU (2.4 GHz).

The reduced excess free energy behaves as

$$f_{ex}(L_0,t)=L_{0,eff}^{-2}h(t[L_{0,eff}/\xi_0]^{1/\nu})+f_s(t), \tag{21}$$

where $L_{0,eff}=L_0+L_s$ with $L_s=1.02(7)$ [25] takes into account corrections due to the Dirichlet boundary conditions and $f_s(t)$ is the surface contribution to the free energy. For a discussion and references see [35]. Taking the derivative with respect to L_0 at $t=0$ we arrive at

$$-\left.\frac{\partial f_{ex}(L_0,t)}{\partial L_0}\right|_{t=0}=2h(0)L_{0,eff}^{-3}=\theta(0)L_{0,eff}^{-3}, \tag{22}$$

where θ is the finite size scaling function of the thermodynamic Casimir force.

It follows

$$\ln z(L_0,\beta_c)=f_{ns}(\beta_c)-\theta(0)L_{0,eff}^{-3}. \tag{23}$$

Note that in the thermodynamic limit the singular part of the free energy density vanishes at the critical point; hence $f_{bulk}(\beta_c)=f_{ns}(\beta_c)$. The results of our fits are given in Table II.

TABLE II. Results for fits with ansatz (23), where we have used $L_s=1.02$ as input. All data for $L_0\geq L_{0,min}$ are fitted. For a discussion see the text.

$L_{0,min}$	f_{ns}	$\theta(0)$	χ^2/d.o.f.
8.5	−0.16315935(9)	−0.0606(3)	0.20
12.5	−0.16315932(10)	−0.0603(6)	0.14
16.5	−0.16315930(12)	−0.0597(17)	0.15

In order to estimate the effect of the error of L_s on our results we have repeated these fits using $L_s=0.95$. For example, for $L_{0,min}=12.5$ we get $f_{ns}=-0.163\ 159\ 30(10)$ and $\theta(0)=-0.0593(5)$. We have also checked the effect of the error of β_c. To this end we have computed $\Delta f(L_0, 0.509\ 150\ 9)$ by using the data for the energy given in table 1 in [35]. We find that the effect on f_{ns} and $\theta(0)$ is small and can be ignored here. Based on the result obtained for $L_{0,min}=12.5$ we take as final results

$$f_{ns}=-0.163\ 159\ 3(1), \quad \theta(0)=-0.060(2), \tag{24}$$

where the error bar covers both the statistical error as well as the error due to the uncertainty of L_s.

This can be compared with the result for ^{4}He films $\theta(0)=-0.07\pm0.03$ [12], the ϵ expansion up to $O(\epsilon)$: $\theta(0)=-0.044$ taken from table I in [14] and the estimate $\theta(0)=-0.062(5)$ obtained from Monte Carlo simulations of the standard XY model [18]. Mon and Nightingale [36] quoted $h(0)\simeq-0.03$ (in their notation Δ^f) as final result. The largest discrepancy is seen for the ϵ expansion. One should note that in [18,21] it has been observed that in the high-temperature phase for $x\gtrapprox 1$ the numerical result for θ matches nicely with the ϵ expansion [14].

B. Free energy density of the bulk system

Here we compute the free energy density of the bulk system for two values of β in the high-temperature phase and two values of β in the low-temperature phase. These results are compared with ones obtained by integrating the energy density starting from $\beta_c=0.509\ 150\ 3$ using the start value $f(\beta_c)=-0.163\ 159\ 3(1)$ obtained above.

For sufficiently large L_0, L_1, and L_2 the quantity $\ln z$ should be a good approximation of the bulk free energy den-

sity. In particular in the high-temperature phase, this should be the case for $L_0, L_1, L_2 \gg \xi_{3D}$. Here we performed simulations at $\beta=0.49$ where $\xi_{2nd,3D}=3.723\,70(19)$ and $\beta=0.5$ where $\xi_{2nd,3D}=6.1498(5)$ (see table 5 in [29]).

At $\beta=0.49$ we have simulated $L_0=49.5$, $L_1=L_2=50$ and $L_0=99.5$, $L_1=L_2=100$. For $L_0=49.5$, $L_1=L_2=50$ we have used block sizes up to $b_1=20$ and $m_l=6$. From 5.2×10^6 cycles we get $f(0.49)=-0.147\,120\,79(18)$. For $L_0=99.5$, $L_1=L_2=100$ we have used block sizes up to $b_1=40$ and $m_l=6$. From 9.5×10^5 cycles we get $f(0.49)=-0.147\,120\,95(17)$. As expected, these results are indeed consistent within error bars and hence a good approximation of the thermodynamic limit.

Based on the experience gained at $\beta=0.49$ we have simulated at $\beta=0.5$ only the lattice size $L_0=99.5$, $L_1=L_2=100$. We have used block sizes up to $b_1=20$ and $m_l=6$. From 6×10^6 cycles we get $f(0.5)=-0.155\,199\,42(24)$.

In the low-temperature phase we find from simulations of a 199.5×500^2 lattice $f(0.533)=-0.189\,318\,67(66)$ and $f(0.56)=-0.226\,936\,25(73)$. We have used blocks up to the size $b_1=80$ and $m_l=6$ for all block sizes. We performed 24 700 and 21 700 cycles for $\beta=0.533$ and $\beta=0.56$, respectively. Both of these simulations took about 8 weeks of CPU time on a single core of a quad-core Opteron(tm) 2378 CPU (2.4 GHz).

Now we can check whether these results for the free energy density are consistent with those obtained from integrating the energy density [30] using Eq. (8).

In [30] we have computed the energy density of the three-dimensional bulk system in the range of inverse temperatures $0.49\leq\beta\leq0.58$. We have fitted these data in the range $0.49\leq\beta\leq0.529$ with the ansatz

$$E(\beta) = E_{ns} + C_{ns}(\beta-\beta_c) + a_{\pm}|\beta-\beta_c|^{1-\alpha} + d_{ns}(\beta-\beta_c)^2 + b_{\pm}|\beta-\beta_c|^{2-\alpha}, \quad (25)$$

where E_{ns}, C_{ns}, $\beta_c=0.509\,150\,3(6)$, and $\alpha=-0.0151(3)$ [22] are input and $a_{\pm}$, d_{ns}, and $b_{\pm}$ are the five free parameters of the fit. For $\beta<0.529$ we have integrated this ansatz using the results for the fit parameter obtained in [30]. In all cases we have taken $\beta_0=\beta_c=0.509\,150\,3$ as starting point of the integration, where we have used the estimate of $f(\beta_c)$ obtained above. Our results are summarized in Table III. For $\beta>0.529$ we performed a numerical integration of the energy density using the trapezoidal rule, starting from $\beta_0=0.52$.

TABLE III. Numerical results for the free energy density of the bulk system. These were obtained by integration of the energy density. As starting point of the integration we have taken the critical point β_c and the value $f(\beta_c)$ obtained in Sec. IV C. In addition in the third column we give estimates of the free energy density obtained directly with the method discussed in the present work.

β	f integral	f direct
0.49	−0.1471210(1)	−0.1471210(2)
0.50	−0.1551994(1)	−0.1551994(2)
0.51463	−0.1684460(1)	
0.52	−0.1740847(1)	
0.52348	−0.1779533(1)	
0.5301	−0.1857405(1)	
0.533	−0.1893183(1)	−0.1893187(7)
0.53814	−0.1958961(2)	
0.54	−0.1983478(2)	
0.54432	−0.2041851(2)	
0.56	−0.2269362(2)	−0.2269363(7)

The estimate for $f(0.52)$ is taken from Table III. We have checked that our result virtually does not depend on the choice of β_0, where we switch from the integration of ansatz (25) to the numerical integration of the energy density. Also the results for $\beta>0.529$ are given in Table III. The error quoted is dominated by the error for the free energy at β_c.

In Table III we also give our results for the free energy density of the bulk system at $\beta=0.49$, 0.50, 0.533, and 0.56 as computed by the method discussed here. We find that the results are consistent within error bars. This confirms that we can indeed compute the free energy density of the bulk system with six to seven accurate digits.

C. Films of the thickness $L_0=8.5$

We have simulated at $\beta=0.52, 0.533, 0.54, 0.56$ in the low-temperature phase of the three-dimensional system. We have taken lattices of the sizes $L_1=L_2=50$, 100, 250, 500, and 1000 to control corrections to the two-dimensional thermodynamic limit of the thin film. The simulations for $L_1=L_2=1000$ took about 18 days of CPU time each. In Table IV we give our results for $-\Delta f_{ex}$, where we have used the

TABLE IV. Numerical results for $-\Delta f_{ex}$ of films of the thickness $L_0=8.5$. In the last row we give the results in [21] for comparison.

$L_1=L_2/\beta$	0.52	0.533	0.54	0.56
50	−0.0007423(14)	−0.0014878(23)	−0.0010417(27)	−0.0003621(23)
100	−0.0007432(8)	−0.0015797(13)	−0.0011867(18)	−0.0003870(13)
250	−0.0007436(5)	−0.0015845(8)	−0.0012564(14)	−0.0003934(8)
500	−0.0007439(3)	−0.0015863(5)	−0.0012679(10)	−0.0003940(5)
1000	−0.0007433(3)	−0.0015846(5)	−0.0012666(11)	−0.0003945(6)
Ref. [21]	−0.0007392(18)	−0.0015795(24)	−0.0012600(26)	−0.0003874(28)

TABLE V. The position β_{min} of the minimum of the Casimir force and its value $-\Delta f_{ex,min}$ as a function of the thickness L_0. In the present work we have completed the table by adding $\Delta f_{ex,min}$ for L_0=6.5, 7.5, 9.5, 12.5, and 24.5. These results are marked by an asterisk.

L_0	β_{min}	$-\Delta f_{ex,min}$
6.5	0.54432(2)	−0.0032744(13)*
7.5	0.53814(2)	−0.0022305(11)*
8.5	0.53354(2)	−0.001582(3)
9.5	0.53010(2)	−0.0011714(8)*
12.5	0.52348(2)	−0.0005468(6)*
16.5	0.51886(2)	−0.0002494(11)
24.5	0.51463(2)	−0.0000803(3)*
32.5	0.51279(2)	−0.0000348(5)

estimates of f_{bulk} computed in Sec. IV B. At β=0.52 the results for all choices of $L_1=L_2$ are consistent within error bars. At β=0.533 a clear deviation of the results from those obtained for larger lattices can be observed up to $L_1=L_2$ =100. The result for $L_1=L_2$=500 deviates by a bit more than two standard deviations from that for $L_1=L_2$=1000, while the results for $L_1=L_2$=250 and $L_1=L_2$=1000 are consistent within error bars. For β=0.54 and β=0.56 the results obtained for $L_1=L_2$=250, 500, and 1000 are consistent within error bars. We conclude that in all cases for $L_1=L_2$=1000 the deviation from the thermodynamic limit is smaller than the error bar.

For comparison we give in the last row results [21] which were obtained by numerical integration of Monte Carlo data for ΔE_{ex}. We see that the results in [21] are by about 4 $\times 10^{-6}$ larger than our present ones. This deviation is about twice the statistical error. In [21] we have started the integration at β=0.49 for L_0=8.5, setting $\Delta f_{ex}(0.49)=0$. From the ϵ expansion [14] we get $\theta(x)\approx -3.9\times 10^{-3}$ for $x=t[L_{0,eff}/\xi_0]^{1/\nu}$ corresponding to β=0.49 and L_0=8.5. Hence $-\Delta f_{ex}=\theta L_{0,eff}^{-3}\approx -4.1\times 10^{-6}$ which fully explains the difference observed in Table IV.

D. Minimum of the Casimir force

In [21] we have determined the position of the minimum of θ for a large number of thicknesses of the film. To this end we have determined the zero of

$$\Delta E_{ex}(L_0,\beta)=E(L_0+1/2,\beta)-E(L_0-1/2,\beta)-E_{bulk}(\beta), \tag{26}$$

where $E(L_0+1/2,\beta)$ is the energy per area of a film of the thickness $L_0+1/2$ and $E_{bulk}(\beta)$ is the energy density of the three-dimensional bulk system. We had simulated at a few values of β in the neighborhood of β_{min}. To get a preliminary estimate of β_{min} we used the information gained already from the simulations for L_0=8.5, 16.5, and 32.5, where we have simulated a large range of β values and the ansatz $\beta_{min}(L_0)-\beta_c\propto L_{0,eff}^{-1/\nu}$. These results are given in Table V, which we have copied from table 2 in [21]. In the present work, we have added the values of θ_{min} for L_0=6.5, 7.5, 9.5, 12.5, and 24.5 that were missing in [21]. To this end, we have simulated lattices of the sizes $L_1=L_2$=500 for L_0=6.5 and 7.5, $L_1=L_2$=1000 for L_0=9.5 and L_0=12.5, and $L_1=L_2$ =2000 for L_0=24.5. From these simulation we get ln z, while f_{bulk} is taken from Table III. Our results for $-\Delta f_{ex}$ are given in Table V.

TABLE VI. We have fitted the minimum of the thermodynamic Casimir force with ansatz (27).

$L_{0,min}$	θ_{min}	L_s	χ^2/d.o.f.
6.5	−1.299(2)	0.849(5)	2.64
7.5	−1.305(3)	0.864(7)	1.64
8.5	−1.313(5)	0.889(13)	0.89
9.5	−1.310(5)	0.880(15)	0.34
12.5	−1.312(9)	0.888(33)	0.50

Let us briefly discuss the simulation of the L_0=24.5 film: the simulations took about 2 months of CPU time on a single core of a quad-core Opteron(tm) 2378 CPU (2.4 GHz). We performed 33 000 update cycles. We have used block sizes up to b_1=160 and m_l=6 for all block sizes.

First we have fitted the results for $-\Delta f_{ex,min}$ given in the third column of Table V with the ansatz

$$-\Delta f_{ex,min}=\theta_{min}(L_0+L_s)^{-3}, \tag{27}$$

where θ_{min} and L_s are the free parameters of the fit. Our results are summarized in Table VI.

The χ^2/degree of freedom (d.o.f.) is smaller than 1 starting from $L_{0,min}$=8.5, where all data with $L_0\geq L_{0,min}$ are included into the fit. We find $L_s\approx 0.89$ which is a bit smaller than our previous result L_s=1.02(7) [25]. Note that already in [21] we observed that L_s=0.95 apparently leads to a better matching of the data than L_s=1.02.

To check the possible effect of subleading corrections we have fitted our data also with the ansatz

$$-\Delta f_{ex,min}=\theta_{min}(1+cL_0^{-2})(L_0+L_s)^{-3}. \tag{28}$$

Note that there are a number of different corrections with a correction exponent close to 2, e.g., $\propto L_0^{-\omega'}$ with ω'=1.8(2) [37] or the restoration of the symmetries that are broken by the lattice. Our results are summarized in Table VII.

Now the value $L_s\approx 0.95$ is fully consistent with our previous result [25]. As final result we quote θ_{min}=−1.31(2), where we have estimated the systematic error by the difference of the two fits [Eqs. (27) and (28)]. This result fully confirms our previous estimate θ_{min}=−1.31(3) [21].

TABLE VII. We have fitted the minimum of the Casimir force with ansatz (28).

$L_{0,min}$	θ_{min}	L_s	c	χ^2/d.o.f.
6.5	−1.322(8)	0.953(3)	1.08(35)	1.13
7.5	−1.320(10)	0.945(5)	0.97(61)	1.40

V. SUMMARY AND CONCLUSION

We have discussed a method to compute the thermodynamic Casimir force in lattice models which is closely related with the one used by de Forcrand and Noth [23] and de Forcrand *et al.* [24] in the study of 't Hooft loops and the interface tension in SU(N) lattice gauge models in four dimensions.

We have tested the method at the example of thin films of the improved two-component ϕ^4 model on the simple cubic lattice. This model shares the XY universality class with the λ transition of ^{4}He. Therefore the Casimir force that is measured for thin films of ^{4}He [12,13] should be governed by the same universal finite size scaling function θ as that computed from lattice models in the XY universality class.

Only quite recently θ has been obtained from Monte Carlo simulations of the standard XY model on the simple cubic lattice [18–20]. This result is of particular interest since other theoretical methods do not provide us with accurate results for θ for the whole range of the scaling variable $x=t[L_0/\xi_0]^{1/\nu}$. Overall one finds a reasonable match between the experimental and Monte Carlo results. In [21] we have redone the Monte Carlo simulations using the improved two-component ϕ^4 model on the lattice. It turns out that there is a discrepancy in the position x_{min} of the minimum of $\theta(x)$: $x_{min}=-5.3(1)$ [18] and $x_{min}=-5.43(2)$ [20] have to be compared with our result $x_{min}=-4.95(3)$ [21].

The purpose of the present work is twofold: first we like to figure out the performance of the method and second we like to check and to complement the results in [21]. In particular, see below.

We have accurately computed the finite size scaling function of the thermodynamic Casimir force $\theta(0)$ at the critical point of the three-dimensional bulk system. Our result is consistent with the experimental result for ^{4}He films [12] and previous Monte Carlo simulations [18,36]. On the other hand there is a clear discrepancy with the ϵ expansion [14].

We have demonstrated that the method even allows us to compute the free energy density of the bulk system. However it seems to be more efficient in this case to integrate the energy density [Eq. (8)].

We have not worked out theoretically how fast $\ln z$ converges to $\lim_{L_1,L_2\to\infty}[f(L_0+1/2,t)-f(L_0-1/2,t)]$. A natural guess is that the convergence is exponentially fast in L_1,L_2 in the high-temperature phase of the film, while in the low-temperature phase it follows a power law. For the thickness $L_0=8.5$ we have simulated at four values of β for a large range of $L_1=L_2$ up to $L_1=L_2=1000$. The results show that the convergence with $L_1,L_2\to\infty$ has no problem in practice. Our final results for $-\Delta f_{ex}$ at these four values of β are consistent but more accurate than those obtained in [21].

Finally we have computed θ_{min} for several thicknesses, where we have taken the values of x_{min} from [21]. This allowed us to improve the estimate $\theta_{min}=1.31(3)$ [21] to $\theta_{min}=1.31(2)$. This part of the study nicely shows that the virtues of the two method are complementary.

We have not worked out theoretically how the numerical effort increases for a given precision with increasing thickness of the film. We also have not optimized the parameters of the algorithm. However it is quite clear from the simulations presented here that the method, using our *ad hoc* choice of the parameters, is superior to the previous proposal [19,20] where only lattices up to the size 40×120^2 had been simulated.

Here we have tested the method at the example of the XY universality class. The application to other universality classes, such as the Ising or Heisenberg universality class, is straightforward. On the other hand, the method seems to be restricted to films with Dirichlet boundary conditions.

ACKNOWLEDGMENT

This work was supported by the DFG under Grant No. HA 3150/2-1.

[1] M. E. Fisher and P.-G. de Gennes, C. R. Seances Acad. Sci., Ser. B **287**, 207 (1978).
[2] K. G. Wilson and J. Kogut, Phys. Rep., Phys. Lett. **12**, 75 (1974).
[3] M. E. Fisher, Rev. Mod. Phys. **46**, 597 (1974).
[4] M. E. Fisher, Rev. Mod. Phys. **70**, 653 (1998).
[5] A. Pelissetto and E. Vicari, Phys. Rep. **368**, 549 (2002).
[6] A. Gambassi, J. Phys.: Conf. Ser. **161**, 012037 (2009).
[7] M. N. Barber, in *Finite-Size Scaling in Phase Transitions and Critical Phenomena*, edited by C. Domb and J. L. Lebowitz (Academic Press, New York, 1983), Vol. 8.
[8] *Finite Size Scaling and Numerical Simulation of Statistical Systems*, edited by V. Privman (World Scientific, Singapore, 1990).
[9] H. W. Diehl, in *Phase Transitions and Critical Phenomena*, edited by C. Domb and J. L. Lebowitz (Academic, London, 1986), Vol. 10, p. 76.
[10] M. Barmatz, I. Hahn, J. A. Lipa, and R. V. Duncan, Rev. Mod. Phys. **79**, 1 (2007).
[11] F. M. Gasparini, M. O. Kimball, K. P. Mooney, and M. Diaz-Avila, Rev. Mod. Phys. **80**, 1009 (2008).
[12] R. Garcia and M. H. W. Chan, Phys. Rev. Lett. **83**, 1187 (1999).
[13] A. Ganshin, S. Scheidemantel, R. Garcia, and M. H. W. Chan, Phys. Rev. Lett. **97**, 075301 (2006).
[14] M. Krech and S. Dietrich, Phys. Rev. A **46**, 1886 (1992).
[15] M. Krech and S. Dietrich, Phys. Rev. A **46**, 1922 (1992).
[16] R. Zandi, A. Shackell, J. Rudnick, M. Kardar, and L. P. Chayes, Phys. Rev. E **76**, 030601(R) (2007).
[17] A. Maciolek, A. Gambassi, and S. Dietrich, Phys. Rev. E **76**, 031124 (2007).
[18] A. Hucht, Phys. Rev. Lett. **99**, 185301 (2007).
[19] O. Vasilyev, A. Gambassi, A. Maciolek, and S. Dietrich, EPL **80**, 60009 (2007).
[20] O. Vasilyev, A. Gambassi, A. Maciolek, and S. Dietrich, Phys. Rev. E **79**, 041142 (2009).

[21] M. Hasenbusch, J. Stat. Mech.: Theory Exp. **2009**, P07031.
[22] M. Campostrini, M. Hasenbusch, A. Pelissetto, and E. Vicari, Phys. Rev. B **74**, 144506 (2006).
[23] P. de Forcrand and D. Noth, Phys. Rev. D **72**, 114501 (2005).
[24] P. de Forcrand, B. Lucini, and M. Vettorazzo, Nucl. Phys. B, Proc. Suppl. **140**, 647 (2005).
[25] M. Hasenbusch, J. Stat. Mech.: Theory Exp. **2009**, P02005.
[26] M. Campostrini, M. Hasenbusch, A. Pelissetto, P. Rossi, and E. Vicari, Phys. Rev. B **63**, 214503 (2001).
[27] M. Hasenbusch and T. Török, J. Phys. A **32**, 6361 (1999).
[28] M. Hasenbusch, J. Stat. Mech.: Theory Exp. **2006**, P08019.
[29] M. Hasenbusch, J. Stat. Mech.: Theory Exp. **2008**, P12006.
[30] M. Hasenbusch, J. Stat. Mech.: Theory Exp. **2009**, P10006.
[31] K. K. Mon, Phys. Rev. Lett. **54**, 2671 (1985).
[32] M. Caselle, M. Hasenbusch, and M. Panero, J. High Energy Phys. **01**, 057 (2003).
[33] U. Wolff, Phys. Rev. Lett. **62**, 361 (1989).
[34] M. Saito, Masters thesis, Hiroshima University, 2007. The numerical program and a detailed description can be found at http://www.math.sci.hiroshima-u.ac.jp/~¿m-mat/MT/SFMT/index.html
[35] M. Hasenbusch, e-print arXiv:0907.2847.
[36] K. K. Mon and M. P. Nightingale, Phys. Rev. B **35**, 3560 (1987).
[37] K. E. Newman and E. K. Riedel, Phys. Rev. B **30**, 6615 (1984).